# Improving the crack propagation response of layered and bonded structures through dissipation mechanisms at different length scales

Federica Daghia, V. Fouquet, L. Mabileau

# Improving the crack propagation response of layered and bonded structures through dissipation mechanisms at different length scales

F. Daghia[a,*], V. Fouquet[a], L. Mabileau[a]

[a] *Université Paris-Saclay, CentraleSupélec, ENS Paris-Saclay, CNRS, LMPS - Laboratoire de Mécanique Paris-Saclay, 91190, Gif-sur-Yvette, France.*

**Abstract**

The wide use of layered and bonded parts in structural applications is limited by the brittle crack propagation response of the weak interface zones. A vast body of literature has focused on the improvement of the bond properties, often proceding with a trial and error approach and without a clear definition of the design requirements in terms of interface properties or structural response. In this work, macroscopic interface properties are defined in terms of Cohesive Zone Models (CZM), and the capital role of the cohesive length in determining the more or less gradual nature of the damage and crack propagation behaviour at the structural level is highlighted through examples on a Double Cantilever Beam (DCB) test. A concept based on a two-mechanisms CZM response with very different cohesive lengths is proposed to ensure a gradual crack propagation behaviour at the structural level, without significantly decreasing the initial damage threshold. A possible strategy to obtain such a macroscale interface response, based on the creation of bridging ligaments, is analysed and the link between the ligament elastic and failure response and the macroscopic interface response are discussed.

*Keywords:* Layered structures, Bonded structures, Cohesive Zone Models,

*Corresponding author

*Email addresses:* federica.daghia@ens-paris-saclay.fr (F. Daghia), vivien.fouquet@ens-paris-saclay.fr (V. Fouquet), lucas.mabileau@ens-paris-saclay.fr (L. Mabileau)

## 1. Introduction

Layered structures, such as laminated composites, are increasingly used in many industrial applications due to their high stiffness and strength to weight ratios. For these types of structures, but also for metallic or multi-material parts, adhesive bonding is an advantageous joining method, as it introduces little extra weight and it does not interfere with the integrity of the substrates, as do other joining methods such as bolts. However, a significant drawback of both laminated composites and bonded joints is the presence within them of extended weak zones in which a crack can rapidly propagate to cause sudden failure of the structure. For this reason, promoting a more gradual crack propagation behaviour for composites and bonded assemblies is a crucial industrial requirement, as well as an active research field.

The weak zones between composite plies or in bonded assemblies can be modelled at the structural (macroscopic) scale as two-dimensional entities, called interfaces, with macroscopic strength and toughness properties. These properties result from the combination of different microscopic phenomena, related to the local three-dimensional material properties and morphology of the crack propagation zone. Many different techniques have been proposed in the literature to improve the macroscopic response of composites and/or bonded interfaces by modifying the local morphology and/or materials contained within the crack propagation zone. Since the early days of composites materials and their use for structural applications, the matrix-rich zones between composite plies have been modified in different ways, by adding fine thermoplastic layers (interlayers) [1] or dispersed particles [2], or by introducing through-thickness reinforcement such as Z-pins [3]. Similar techniques can be found for bonded assemblies, where hybrid joints have been manufactured including different types of particles, fibres, wires or nets [4, 5, 6]. Other strategies for bonded joints do not involve the addition of external material, but the use of heterogeneous surface

preparation to trigger bridging ligaments [7], or the creation of stop holes [5] or sacrificial cracks [8]. Many of these works have experimentally demonstrated a modified mechanical response of the joint, generally presented as an increase of interface fracture toughness and evaluated through standard crack propagation tests, such as the Double Cantilever Beam (DCB), and the associated data reduction methods. However, these works generally proceeded by trial and error, without a clear definition of the design requirements for the interface properties or for the structure's response.

This study is an attempt to formulate clear design requirements for the improvement of the crack propagation response of layered and bonded structures, expressed in terms of the desired macroscopic interface properties. To this aim, Cohesive Zone Models (CZM) [9, 10] are introduced in Section 2.1 to describe the macroscopic behaviour of the interface. In particular, the role of the cohesive length, or process zone size, in defining the type of structural response is highlighted through DCB simulations with different CZM properties. The gradual crack propagation response which one can aim for in the design requires the cohesive length to be similar to the characteristic size of the structure. Achieving such a large cohesive length with a single dissipation mechanism would require an extremely large increase in the fracture toughness, or to decrease the threshold at which interface damage begins, which would be detrimental to the initial structural response. For this reason, in Section 2.2 we investigate the possibility of designing interfaces with a complex behaviour, including dissipation mechanisms with very different cohesive lengths which work in parallel to promote both initial strength and a more gradual damage and crack propagation behaviour at the structural level. It is important to underline that, since the response depends both on the CZM properties and on the structural configuration, the interface behaviour needs to be tailored to the specific structural application under consideration, as illustrated in Section 2.3. The clear definition of the required macroscopic interface properties to achieve a given structural response opens the way to a systematic design approach for improved interfaces, as it is discussed in Section 3, where the interface improvement strategy con-

sisting in the creation of bridging ligaments, proposed in many literature works [11, 4, 5, 7, 6], is interpreted in terms of the required CZM properties. The role and the control of the global and local instabilities and dynamic response appear as a key point for further investigation.

## 2. Design requirements for improved crack propagation response in terms of macroscopic interface properties

### *2.1. Cohesive Zone Models (CZM) and the importance of the cohesive length*

The main aim of this work is to formulate clear design requirements for the improvement of the crack propagation response of layered and bonded structures in terms of macroscopic interface properties. The wide range of structural responses which can be observed during crack propagation can be effectively analysed through the prism of Cohesive Zone Models (CZM) [9, 10]. After their first introduction in the 1960s [12, 13], these models have gained great popularity for their ability to account for crack initiation and propagation, and are now very commonly used in a computational setting to simulate a wide range of structural problems, for instance within composites and bonded structures [14]. Here, we will use them to provide a macroscopic description of the interface behaviour, and to investigate the range of structural responses which can be achieved by modifying the interface properties.

CZM define the mechanical behaviour of an interface as a traction/separation law, relating the stress $\sigma$ to the displacement jump $[\![u]\!]$ between the two sides on the interface. These laws enable us to describe the gradual evolution of the interface state, from healthy to partially damaged to broken, and to quantify the dissipated energy per unit surface of crack creation as the area enclosed in the traction/separation curve. Different types of dissipation can be included in CZM models, only damage is considered in this discussion, for simplicity. As a consequence, a general one-dimensional CZM law reads

$$\sigma = K(1-d)[\![u]\!] \tag{1}$$

$$d = f\left([\![u]\!]\right), 0 < d < 1, \dot{d} \geq 0 \tag{2}$$

It should be noted that this law naturally contains a physically meaningful characteristic length, the thickness of the crack propagation zone $h_i$, since one can recover a standard local constitutive law by considering a homogeneous interface material and loading and setting $K = \frac{E_i}{h_i}$ and $[\![u]\!] = \varepsilon \cdot h_i$.

Choosing different forms for $f([\![u]\!])$ enables us to define different shapes of the traction/separation law (triangular, exponential, rectangular... see [10]). More than by the shape of the law, however, the response of a structure including one or more CZM is governed by the orders of magnitude of its three key parameters [9]:

- $K$, the initial interface stiffness, which is generally high due to the small thickness $h_i$ of the crack propagation zone;
- $\sigma_{max}$, the maximum value of the stress, which, for some law shapes, may not correspond to the stress at damage initiation;
- $G_c$, the dissipated energy per unit surface during crack propagation, also called the critical strain energy release rate or the fracture toughness of the interface.

The maximum displacement jump at failure, $[\![u]\!]_{max}$, can also be considered in alternative to $G_c$, as they are directly related once the other parameters and the shape of the law are defined. Fixing these parameters naturally introduces a second characteristic length in the problem, the cohesive length, or process zone size, that is the length of the transition zone between healthy and completely broken interface:

$$l_c \propto \frac{EG_c}{\sigma_{max}^2} \tag{3}$$

Here, $G_c$ is the energy per unit surface to be dissipated for complete interface failure, $\frac{\sigma_{max}^2}{E}$ is proportional to the maximum elastic energy per unit volume which can be stored in the material surrounding the interface (with Young's modulus $E$), thus the ratio between the two yields the length of the partially damaged zone. This expression for the cohesive length is valid for cracks within

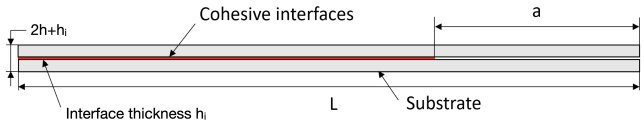


Figure 1: Geometry of the Double Cantilever Beam (DCB) test

massive structures, while for slender structures dominated by bending the cohesive length also depends upon the structural thickness [14].

The ratio between the cohesive length $l_c$ and the characteristic geometric dimensions of the structure $a$, such as the crack length, enables us to distinguish between two different kinds of structural behaviour [9]:

- if $\frac{l_c}{a} \ll 1$, the details of the CZM shape are not significant to the structure's response and crack propagation is governed by the fracture toughness $G_c$ and it can be predicted with standard Linear Elastic Fracture Mechanics (LEFM);

- if $\frac{l_c}{a} \sim 1$, gradual damage development occurs in the interface, and the progress of the crack within the structure depends upon both the structural problem under consideration and the details of the CZM.

In order to illustrate the role of cohesive length in determining the global structural behaviour, we consider here the Double Cantilever Beam (DCB) test, which is often used to characterise the mode I fracture toughness of composites and bonded assemblies. The geometry and material properties for the test are similar to those considered in [7] and they are given in Figure 1 and Tables 1 and 2. Different types of interface behaviours will be considered throughout this work to illustrate the key concepts introduced. All of the finite element simulations discussed in this work were carried out in Abaqus/Standard in a two-dimensional plane strain setting, using linear quadrilateral elements for the substrates and cohesive elements for the interface, with an average mesh size of 0.2 mm. A dissipation-driven arc length method [15] was implemented in the form of a user element to achieve robust convergence of the simulations.

Table 1: Geometrical parameters used in the simulations

| **Geometrical parameters** | **Notations** | **Values** | **Units** |
|---|---|---|---|
| substrates length | $L$ | 240 | mm |
| substrates thickness | $h$ | 2 | mm |
| substrates width | $b$ | 20 | mm |
| initial crack length | $a$ | 50 | mm |
| interfaces thickness | $h_i$ | 0.2 | mm |

Table 2: Elastic properties of the substrates

| **Material parameters** | **Notations** | **Values** | **Units** |
|---|---|---|---|
| longitudinal Young's modulus | $E_1$ | 125 | GPa |
| transverse Young's moduli | $E_{2,3}$ | 7.8 | GPa |
| Poisson's ratios | $\nu_{12,13}$ | 0.33 | - |
| Poisson's ratio | $\nu_{23}$ | 0.4 | - |
| shear moduli | $G_{12,13}$ | 5.1 | GPa |
| shear modulus | $G_{23}$ | 2.8 | GPa |

Three different sets of parameters are initially considered here for simple triangular CZM:

- $K = 7500$ MPa·mm$^{-1}$, $\sigma_{max} = 19$ MPa, $G_c = 0.28$ kJ·m$^{-2}$, which constitutes the baseline response in [7];
- $K = 7500$ MPa·mm$^{-1}$, $\sigma_{max} = 19$ MPa, $G_c = 0.84$ kJ·m$^{-2}$, in order to simulate an increase in the toughness $G_c$ without significant evolution of the cohesive length $l_c$;
- $K = 7500$ MPa·mm$^{-1}$, $\sigma_{max} = 0.19$ MPa, $G_c = 0.84$ kJ·m$^{-2}$, where the maximum stress $\sigma_{max}$ has been artificially decreased in order to significantly increase the cohesive length $l_c$.

It should be noted that here the CZM represents the whole bond, that is the glue plus the interfaces between the glue and the substrate, thus the CZM thickness $h_i$ and its stiffness $K$ have been adjusted accordingly ($K = \frac{E}{h_i}$ where $E$ is the Young's modulus of the glue and $h_i$ is its thickness). The choice of a simple triangular law is taken to represent a single dissipation mechanism,

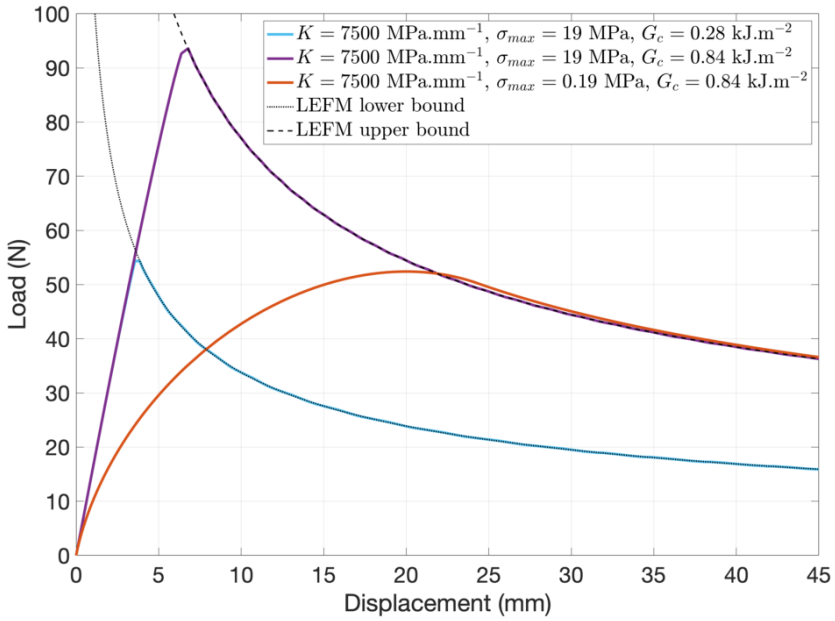


Figure 2: DCB responses for different cohesive lengths

whose microscopic origins are not detailed for the time being. The DCB response for each of the three laws are represented in Figure 2. The analytical LEFM prediction, based on a simple beam model, is also depicted for the two different values of toughness, $G_c = 0.28$ kJ·m$^{-2}$ and $G_c = 0.84$ kJ·m$^{-2}$.

As it can be observed, increasing the fracture toughness $G_c$ by a factor 3 increases the load value at which crack propagation starts to occur, but it results in an analogous crack propagation curve with sharply decreasing load, in agreement with classical LEFM results. Increasing the fracture toughness and the cohesive length (through an artificial decrease of the maximum stress $\sigma_{max}$), on the other hand, results in a more gradual damage development and crack propagation behaviour at the structural level, however the damage starts to occur much too early, due to the very low value of $\sigma_{max}$. Neither of the two structural responses is optimal: in the first case, the toughness increase alone does not suffice to modify the post-peak response with rapidly decreasing force, while in the second case the damage starts much too early, even though

it progresses in a more gradual way. A structural response with initial damage threshold analogous or higher then the baseline curve, but followed by a more gradual damage and crack propagation behaviour, ideally under increasing or constant load, is defined here as the target behaviour to be achieved, as it would correspond to a safer and more damage tolerant type of response. Obviously, the type of structural response depends primarily on the structural configuration (geometry, material properties, loading, bond position, initial crack length). However, the CZM properties, and in particular the cohesive length associated to its key parameters, play a significant role in defining the type of structural response, as it was discussed here.

Obtaining a gradual post-peak crack propagation response without triggering early damage development and using a single dissipation mechanism would require an extremely large increase of the interface toughness. In the following, the possibility of triggering multiple dissipation mechanisms, each with its own, different cohesive length, is explored, resulting in complex-shaped CZM as those discussed in [10].

### *2.2. Complex CZM with multiple dissipation mechanisms*

Let us consider two different dissipation mechanisms, each described for simplicity by a simple triangular CZM with specific values of $K$, $\sigma_{max}$ and $G_c$. We further suppose that the two mechanisms are able to dissipate a similar amount of energy (that is, that their values of $G_c$ are similar), but their maximum stresses $\sigma_{max}$ are significantly different, resulting in very different cohesive lengths (Figure 3(a)). If these two mechanisms are set to work in parallel, the overall response of the resulting CZM would be similar to the one described in [10], and illustrated in Figure 3(b): the initial damage phase, dominated by the mechanism with short cohesive length, would be followed by the activation of the mechanism with long cohesive length, which would provide a more gradual post-peak response. Of course, the main challenge in conceiving interface microstructures that display such complex behaviour is that the two mechanisms must be working in parallel: indeed, if they worked in series (as it would be the

case, for instance, if the two represented CZM corresponded to the glue and to the glue/substrate interface behaviours, respectively), the overall CZM response would be dominated by the mechanism with the lowest maximum stress $\sigma_{max}$ (see Figure 3(c)).

The effect of such complex, two-mechanisms CZM on the structural response of the DCB test, considered previously, is discussed in the following. In order to model the complex CZM in Abaqus without implementing a user material, the interface is represented by two superposed parts, joined at the top and bottom with tie constraints, each containing cohesive elements whose law represents one of the two dissipation mechanisms working in parallel.

Different choices of CZM, as well as the associated DCB responses, are depicted in Figures 4 and 5. In particular, the short cohesive length mechanism is kept constant throughout this study, and equal to the baseline mechanism considered in Section 2.1, while the role of $\sigma_{max}$ and $K$ of the long cohesive length mechanisms are investigated through a parametric study (the CZM parameters for each case are given in the Figures). The analytical LEFM prediction, based on a simple beam model, is also depicted for two different values of toughness $G_c$, corresponding to the short cohesive length mechanism alone, as well as to the total energy dissipated by the two mechanisms.

As it can be observed, the load value at which crack propagation starts is governed by the short cohesive length mechanism: in particular, it is the same as the baseline response depicted in Figure 2, as the short cohesive length mechanism was supposed identical to the baseline response. The post-peak response, on the other hand, is strongly influenced by the parameters of the long cohesive length mechanism. In particular, for a fixed $G_c$, $\sigma_{max}$ determines the cohesive length, which controls the level of displacement at which the curve rejoins the LEFM response corresponding to the total toughness of the two mechanisms. At this stage, marked by the cross in Figures 4(c) and 5(c), the process zone for the long cohesive length mechanism has completely developed, and its size is comparable to the crack size and much larger than the specimen thickness (see Figure 6 for the plot of the damage parameter value along the

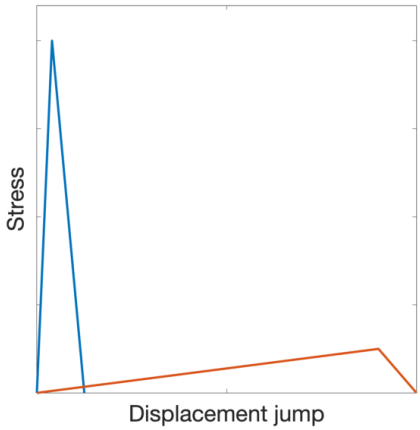


(a) Dissipation mechanisms with different cohesive lengths

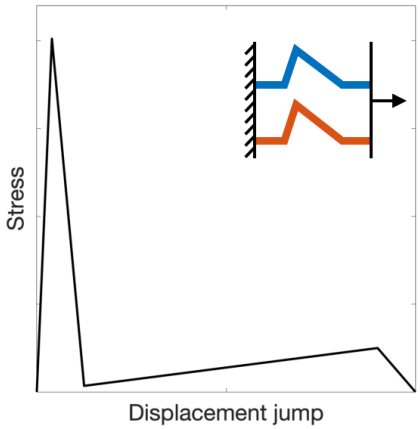


(b) Overall CZM response for two mechanisms working in parallel

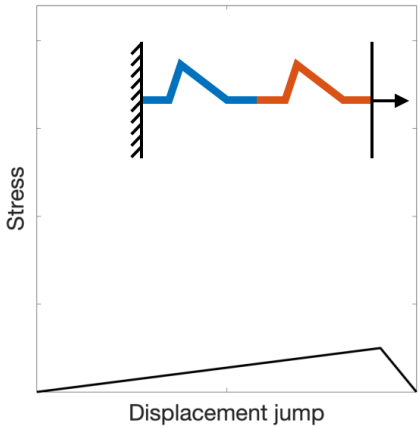


(c) Overall CZM response for two mechanisms working in series

Figure 3: Complex CZM with multiple dissipation mechanisms

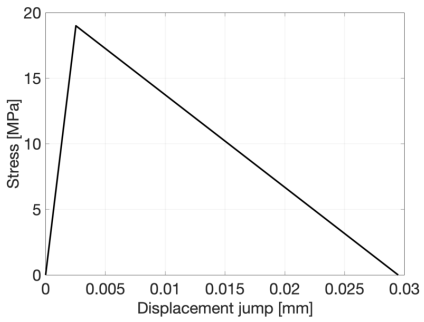


(a) CZM short cohesive length law

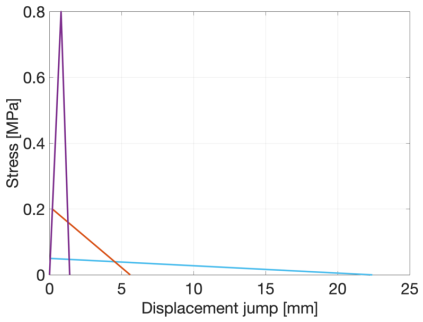


(b) CZM long cohesive length laws

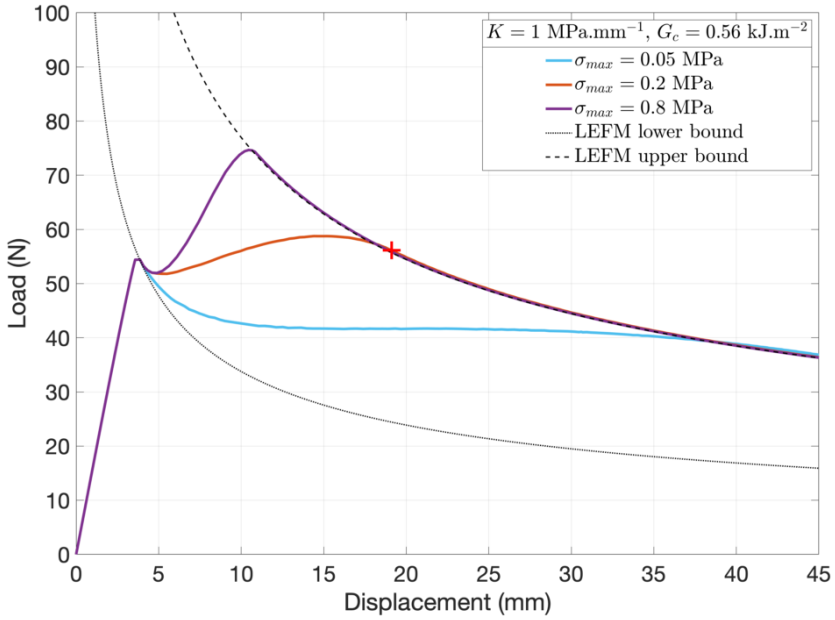


(c) DCB responses

Figure 4: CZM laws and DCB responses for different complex, two-mechanisms CZM: role of $\sigma_{max}$ for the long cohesive length mechanism (the colour of the DCB curves correspond to the colour of the implemented CZM)

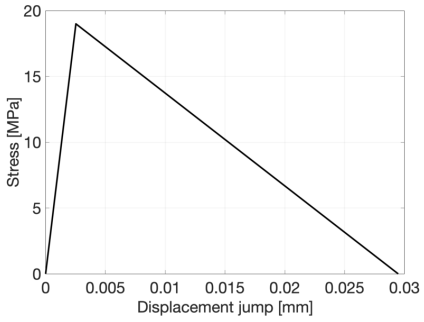


(a) CZM short cohesive length law

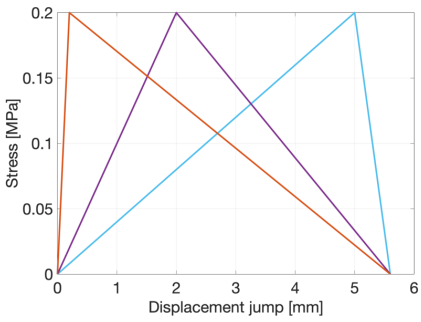


(b) CZM long cohesive length laws

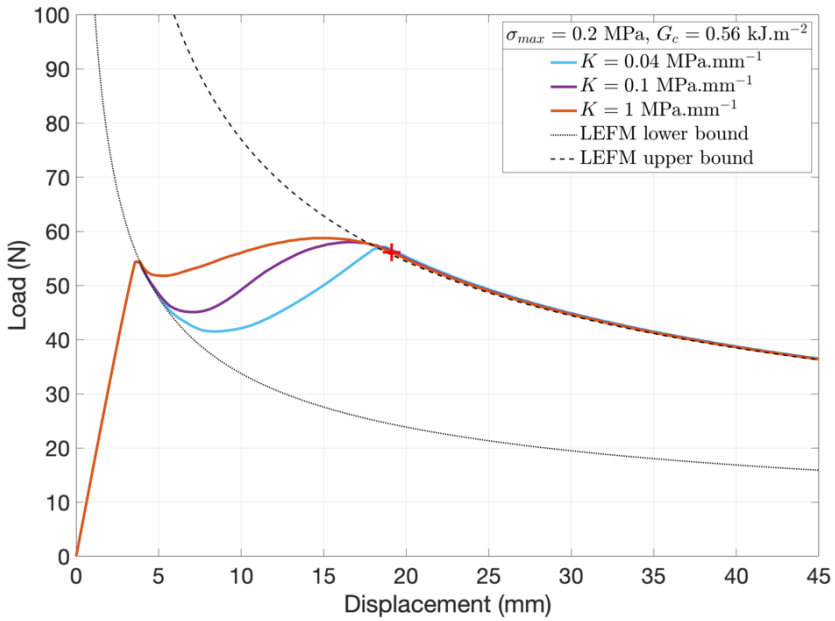


(c) DCB responses

Figure 5: CZM laws and DCB responses for different complex, two-mechanisms CZM: role of $K$ for the long cohesive length mechanism (the colour of the DCB curves correspond to the colour of the implemented CZM)


Figure 6: Cohesive length $l_c$ for the long cohesive length mechanism ($K = 1$ MPa·mm$^{-1}$, $\sigma_{max} = 0.2$ MPa, $G_c = 0.56$ kJ·mm$^{-2}$, geometry and material from [7], displacement amplifying factor 1)

interface for the long cohesive length mechanism).

On the other hand, $K$ controls the shape of the curve between these two points, with higher initial stiffness resulting in improved post-peak response. The effect of the different parameters of the long cohesive length CZM on the DCB structural response are summarised in Figure 7.

The analyses presented in this Section illustrate the role of a two-mechanisms CZM to promote a gradual crack propagation behaviour at the structural level, while maintaining the initial damage threshold of the original one-mechanism interface response. The relatively few parameters of the two-mechanisms CZM law can be used to formulate design requirements in terms of macroscopic interface properties, which in turn can be used as guidelines to design microscopic bond features with the desired macroscopic response. The example of the interface improvement strategy based on the creation of multiple bridging ligaments, proposed in many literature works [11, 4, 5, 7, 6], is analysed through this prism in Section 3.

As it was already pointed out in Section 2.1, the computed structural responses depend on both the structural configuration (geometry, material properties, loading, bond position, initial crack length) and the CZM properties. For this reason, the interface behaviour should not be considered and optimised on its own, but in conjunction with the targeted structural application, if a gradual crack propagation behaviour at the structural level is to be obtained. This aspect is illustrated in the following, by considering the DCB configuration from

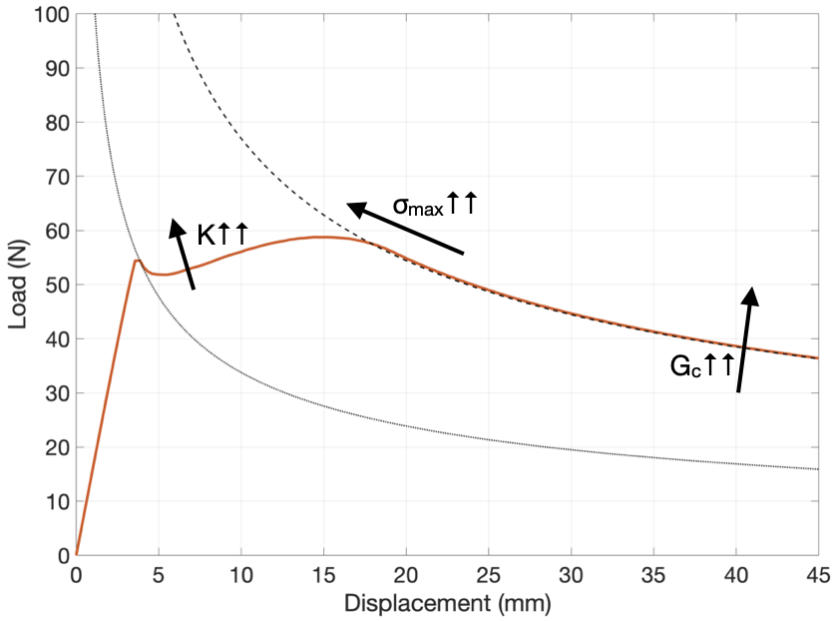


Figure 7: Effect of the different parameters of the long cohesive length CZM on the DCB response

[5], involving different geometry and material properties, together with the same two-mechanisms CZM as considered in this Section. The study of the effect of a two-mechanisms CZM on structural configurations different from the DCB is the subject of ongoing work. It is anticipated that structural configurations with highly unstable crack propagation behaviour would have little or no benefit from the existence of the long cohesive length mechanism, as pointed out in [10].

### *2.3. The role of the structural configuration*

In order to illustrate the combined role of the structural configuration and of the CZM parameters, the two-mechanisms CZM discussed in the previous Section was applied to a DCB with different geometry and material, from [5]. Here, the substrates material is aluminium, the thickness of each arm is $h = 21$ mm and their width $b = 12.8$ mm, while the precrack is $a = 30$ mm long. The CZM properties are the same as those discussed before, with the short cohesive length mechanism being equal to the baseline and the long cohesive

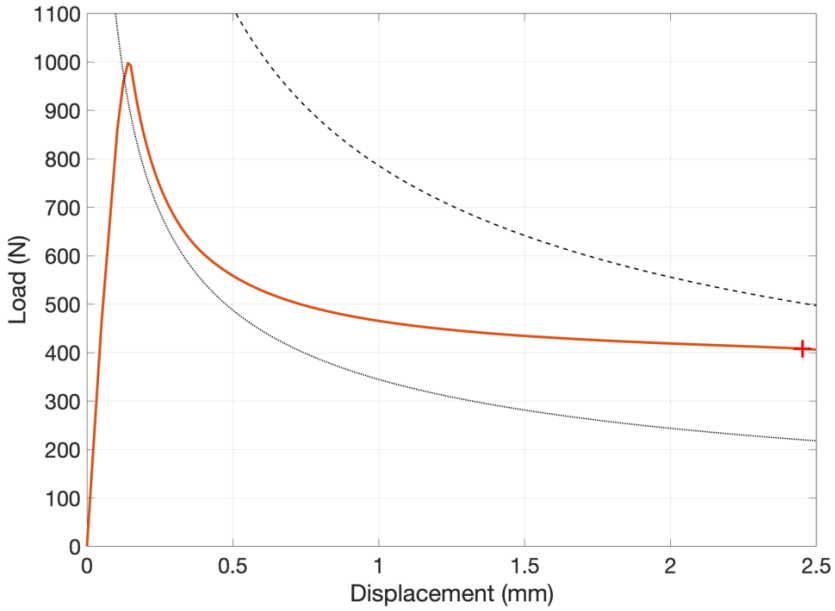


Figure 8: Global response for the DCB geometry and material from [5] and the two-mechanisms cohesive law considered here ($K = 1$ MPa·mm$^{-1}$, $\sigma_{max} = 0.2$ MPa, $G_c = 0.56$ kJ·mm$^{-2}$)

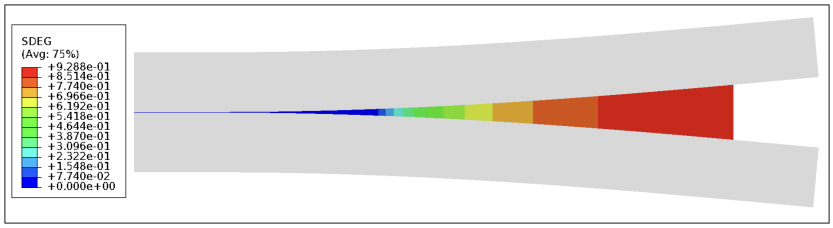


Figure 9: Long cohesive length mechanism towards the end of the simulation ($K = 1$ MPa·mm$^{-1}$, $\sigma_{max} = 0.2$ MPa, $G_c = 0.56$ kJ·mm$^{-2}$, geometry and material from [5], displacement amplifying factor 10)

length mechanisms corresponding to the red curve in Figures 4(c) and 5(c). The DCB response is plotted in Figure 8, while the damage parameter along the interface for the long cohesive length mechanism at the instant marked by the cross is plotted in Figure 9.

The greater thickness of the DCB arms obviously leads to much larger loads and smaller displacement at the beginning of crack propagation. The post-peak response is still contained between the two LEFM bounds, but it does not reach the upper bound curve before the crack reaches the end of the specimen. Indeed, as it can be seen in Figure 9, the long cohesive length mechanism has not completely developed towards the end of the simulation. While the curve associated to the two-mechanisms CZM is above the LEFM lower bound, the load still decreases significantly at the beginning of crack propagation, and it stabilises only later at a load about half the peak one. The improvement of the overall structural response brought about by the development of the same long cohesive length mechanism is much less significant for this structural configuration than for the one investigated by [7].

This example is important to show that the optimisation of the CZM response should not be considered on its own, but together with the structural configuration of interest, if the design requirement is to obtain an improved progressive crack propagation response at the structural level.

## 3. Design of the microscopic bond features to achieve a two-mechanisms CZM response: the example of bridging ligaments

In the previous Section, the effectiveness of a two-mechanisms CZM to ensure both initial damage resistance and a more gradual post-peak crack propagation was demonstrated on a composite Double Cantilever Beam example. In particular, it was shown that the initial crack propagation is controlled by the toughness associated to the short cohesive length mechanism through standard LEFM considerations, while the post-peak response depends on both the long cohesive zone mechanism and the structural configuration. In this section,

the development of bridging ligaments is discussed as a possible strategy to design microscopic bond features that result in the desired macroscopic interface properties.

For small displacement jumps, the enhanced bond should retain analogous, or improved, strength and toughness properties with respect to the baseline bond (short cohesive length mechanism). For larger displacement jumps, on the other hand, a low stiffness, low stress bond response should be developed. In order for this second mechanism to dissipate a similar amount of energy as the short cohesive length mechanism, the maximum displacement jump at failure should be rather large. In the following discussion, we retain the orders of magnitude of the examples discussed in the previous Section:

- $\sigma_{max} = 0.1 - 0.5$ MPa;
- $G_c = 0.25 - 1$ kJ/m$^2$;
- $[\![u]\!]_{max} = 1 - 20$ mm.

These should not be intended as material properties, but as the average macroscopic response resulting from complex microscopic bond features.

### *3.1. Microscopic mechanisms during ligament creation, loading and failure*

A possible solution to achieve this type of response is by promoting the formation of bridging ligaments across the bond. In laminated composites, the fibres contained within the plies may tend to cross the matrix-rich interface region, especially for delamination between unidirectional plies having the same fibres orientation [16, 17, 11], therefore they need to be broken or pulled out during crack propagation. According to the DCB composites standards [16, 17], the R-curve effect and increased toughening related to bridging fibres should not be considered in the bond fracture toughness, as it does not typically occur for delamination of $[\alpha/\beta]$ interfaces. On the other hand, a finer exploitation of the DCB test data makes it possible to identify the associated CZM, resulting in macroscopic responses with orders of magnitude analogous to those

quoted above [11]. A possibility to exploit this bridging effect to improve the delamination response of $[\alpha/\beta]$ interfaces is to include a fine layer of long fibres, eventually in the form of mat, within the interfaces [4]. The creation of bridging ligaments in bonded structures can follow similar principles, based on the manufacturing of hybrid joints including wires or meshes within the bond [5, 6], or it can be promoted by the heterogeneous surface treatment of the bonding surfaces, which creates trapping sites for the crack and results in the creation of glue ligaments [7]. In [5], in particular, the macroscopic CZM response was measured experimentally through tensile tests on the bond, and a two-mechanism CZM with orders of magnitude similar to those quoted above was identified.

A step further from these trial and error concepts would be to optimise the microscopic bond features in order to achieve the desired macroscopic interface response, which can result in the targeted gradual crack propagation at the structural level. In the following, the link between the microscopic bond features and its macroscopic response are discussed in qualitative term, considering a schematic microscopic model with a single ligament. Fine modelling and simulation of the microscopic bond response to obtain numerically the homogenised macroscopic CZM properties is currently a work in progress.

In the initial stage of loading, the healthy bond is stiff due to its small thickness, and a low displacement jump leads to crack initiation and propagation in the brittle phase of the bond, with a similar response to the baseline, unreinforced bond (Figure 10(a)). The presence of trapping sites due to heterogeneous surface treatment, or the presence of wires or meshes within the joint, causes the crack to jump and create a ligament, which remains as the only load carrying element across the bond (Figure 10(b)). The macroscopic response with low stiffness, low stress and large displacement, required to achieve a long cohesive zone, is related to the choice of the ligament material, but also to its small cross-section with respect to the projected bond area and to its bending and rotation-dominated kinematics. Finally, in the last stage of loading, ligament failure occurs (Figure 10(c)).

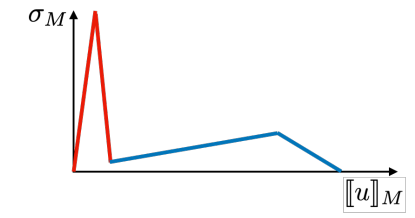


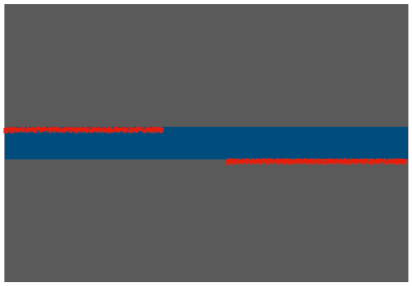

(a) Failure of the brittle phase of the bond

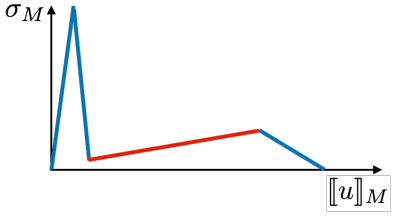


(b) Creation and loading of the ligament

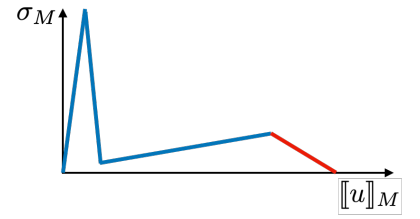


(c) Failure of the ligament

Figure 10: Schematic description of the microscopic failure mechanisms in the presence of bridging ligaments

*3.2. Energy dissipation, dynamics and instability: the role of ligament failure*

The type of ligament failure strongly depends on the ligament material and anchoring conditions, and it is essential to ensure the extra energy dissipation required for real bond properties enhancement. Indeed, while a portion of the extra dissipated energy is related to the increase in the cracked surface of the brittle phase of the bond, since the crack runs on either side of the ligament, a significant energy dissipation is necessary during the ligament failure stage in order to limit global and local dynamic and instability effects.

Different types of ligament failure can be expected:

1. sudden, brittle failure of the ligament or of the ligament anchoring, where the stored elastic energy in the ligament is larger than the energy dissipated at failure (as in [7]);
2. progressive, ductile failure of the ligament material, where the energy is dissipated through phenomena such as plastic stretching and necking (as in [5]);
3. progressive, ductile failure of the ligament anchoring, where the energy is dissipated through interface failure and friction during ligament pull-out (as in typical fibres bridging situations in composites delamination).

In order to sketch the type of macroscopic CZM behaviour which can be expected during stages 2 and 3 for each type of ligament failure, let us consider the simplified case of a straight elastic ligament under tension, depicted in Figure 11. The macroscopic bond response (index $M$) during the loading stage 2, controlled by the elastic behaviour of the ligament can be computed in terms of the ligament material, geometry and local stress/strain response (index $m$) as

$$\sigma_M = \sigma_m \frac{S_l}{S_b}, \quad [\![u]\!]_M = \varepsilon_m \cdot L = \sigma_M \frac{S_b L}{S_l E} = \frac{\sigma_M}{K_M}, \tag{4}$$

where $\sigma_m$ and $\varepsilon_m$ are the (uniform) stress and strain in the ligament, $L$ is the length of the ligament, $E$ its Young's modulus and $S_l$ its cross-section, while the bond area affected by the ligament is denoted by $S_b$. The energy density

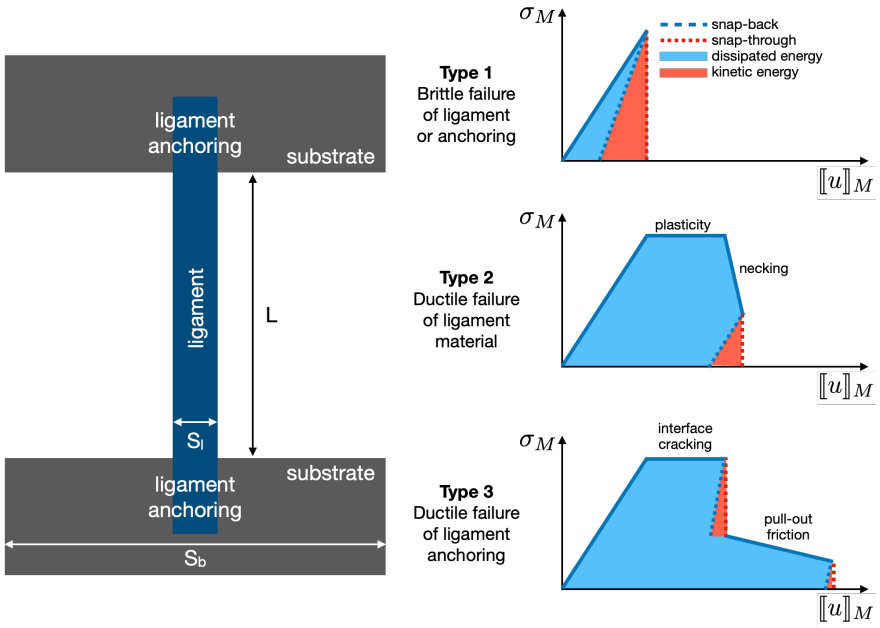


Figure 11: Microscopic features and macroscopic bond behaviour for different ligament failure conditions

per unit projected bond surface stored in the ligament during its elastic loading thus reads

$$E_{el} = \frac{1}{2}\sigma_M [\![u]\!]_M = \frac{1}{2}\frac{\sigma_M^2}{K_M}. \tag{5}$$

In ligament failure Type 1, the ligament or its anchoring experience a sudden, brittle failure at a given macroscopic stress level $\sigma_{M,max}$. In this case, the energy dissipated during ligament failure $E_d$ is smaller than the stored elastic energy $E_{el,max}$, and the static equilibrium curve for the macroscopic bond response displays a snap-back behaviour (Figure 11, top). A displacement driven curve, on the other hand, results in a snap-through response, where the extra energy contribution is in the form of kinetic energy release. If the kinetic energy released is significant, this type of situation cannot be accurately modelled using the static CZM modelling approach introduced here, and it requires to account for dynamic effects. Furthermore, depending on the amount of kinetic energy released, the locally unstable response may trigger a global instability of

the force-displacement structural response, as observed in [7]. Such an unstable response is in contrast with the sought-for gradual post-peak crack propagation, thus the introduction of ligaments displaying brittle failure with a significant release of kinetic energy may not result in an improvement of the crack propagation behaviour according to the definition adopted in this paper.

In ligament failure Type 2, on the other hand, the ductile response of the ligament material results in a plateau during plastic stretching of the ligament, followed by softening then failure due to plastic localisation (necking) (Figure 11, middle). While some local instabilities can still be observed during the final stages of loading, the behaviour is much more progressive, with a greater ratio of energy dissipation to energy release. This type of behaviour, observed for instance in [5], should lead to a better control of local and global dynamics, and therefore to the gradual crack propagation behaviour sought for.

Finally, in ligament failure Type 3, failure of the anchoring is expected to occur in two phases: first, cracking of the interface between the ligament and the substrate, followed by frictional energy dissipation during pull-out of the ligament as described, for instance, in [18] (Figure 11, bottom). Depending on the characteristics of the ligament, the substrate and the interface, as well as on the length of the embedded parts of the ligament, rather different pull-out responses can be observed, which may or may not include significant dynamic energy release. The progressive failure behaviour sought for can be obtained for appropriate configurations.

Ligament failures Types 2 and 3, therefore, seem to have more potential to provide the required extra energy dissipation and lead to the sought-for gradual crack propagation behaviour. Indeed, similar strategies are regularly used to improve the material ductility in contexts other than bonded structures, for instance by introducing metallic fibres to slow down the crack propagation of concrete in tension (Type 2 situation, [19]) or by promoting crack deviation at the fibre/matrix interfaces in Ceramic Matrix Composites (Type 3 situation, [20]). Differently from the present case, these two examples aim at improving the bulk material, rather than a weak interface, cracking properties.

*3.3. Ligaments density and variability*

While a single ligament was considered in the discussion up to now, the ligaments distribution and variability also play a crucial role in the crack propagation response. Concerning the ligaments distribution, while the presence of small, densely distributed ligaments can be effectively modelled as an equivalent macroscopic CZM, the effect of few, distant ligaments is best described with discrete cohesive "springs", similar to those considered in [21]. As it was shown in [22, 21], the denser the ligaments are, the more ligaments are active simultaneously during crack propagation, resulting in a more progressive and stable global behaviour. On the other hand, few large ligaments may result in multiple global instabilities, one for each ligament failure, even if the local ligament behaviour is stable. Since, in the framework of long cohesive length mechanisms, the global response depends on the combination of the bond and the structure's properties, notions such as the ligament density should also be put in perspective with respect to the targeted structural configuration.

The role of ligaments variability on the global structural response, on the other hand, is not so clear in the literature, with different proposed strategies promoting either random or regular ligaments creation. These two strategies may differ in terms of global structural response, but also in terms of the required technical and manufacturing efforts towards the creation of an enhanced bond. The CZM modelling approach discussed in this paper, eventually completed with a discrete bridging vision similar to [21] and an appropriate description of dynamic effects, could play a very important role in the understanding of the role of these multiple microscopic bond features.

## 4. Conclusions and perspectives

This study aims at defining clear design requirements for the improvement of the crack propagation response of layered and bonded structures, in terms of macroscopic interface properties. To this end, Cohesive Zone Models are considered as a relatively simple way to describe the macroscopic behaviour

of an interface, comprising different dissipation mechanisms. In particular, it is shown that the presence of two dissipation mechanisms with very different length scales can effectively produce a more gradual post-peak response for the Double Cantilever Beam test considered here, without significantly modifying the initial damage threshold. The reinforcement strategy consisting in the creation of bridging ligaments, proposed in many literature works, is analysed through this prism. In particular, the role of the ligament failure in triggering energy dissipation, versus kinetic energy release leading to dynamic instabilities, is qualitatively analysed for different types of ligament failure. Perspectives of this work include a detailed analysis of the local and global dynamic effects and the related instabilities, a finer microscopic description of the mechanisms at work in ligament creation in order to obtain numerically the macroscopic interface properties, as well as the applicability of this reinforcement concept to structural configurations other than the DCB.

**Acknowledgements**

The authors would like to acknowledge Dr. Christophe Cluzel for the useful discussions, and Dr. Emmanuel Baranger for sharing the development of the dissipation-driven algorithm in Abaqus.

**References**

[1] J. E. Masters, Improved impact and delamination resistance through interleafing, Key Engineering Materials 37 (1989) 317–347.

[2] M. R. Groleau, Y.-B. Shi, A. F. Yee, J. L. Bertram, H. J. Sue, P. C. Yang, Mode ii fracture of composites interlayered with nylon particles, Composites Science and Technology 56 (1996) 1223–1240.

[3] A. P. Mouritz, Review of z-pinned composite laminates, Composites: Part A 38 (2007) 2383–2397.

[4] A. J. Kinloch, A. C. Taylor, The toughening of cyanate-ester polymers, Journal of Materials Science 37 (2002) 433–460.

[5] K. Maloney, N. A. Fleck, Toughening strategies in adhesive joints, International Journal of Solids and Structures 158 (2019) 66–75.

[6] A. Yudhanto, M. Almulhim, F. Kamal, R. Tao, L. Fatta, M. Alfano, G. Lubineau, Enhancement of fracture toughness in secondary bonded cfrp using hybrid thermoplastic/thermoset bondline architecture, Composites Science and Technology 199 (2020) 108346.

[7] R. Tao, X. Li, A. Yudhanto, M. Alfano, G. Lubineau, Laser-based interfacial patterning enables toughening of CFRP/epoxy joints through bridging of adhesive ligaments, Composites: Part A 139 (2020) 106094.

[8] A. Wagih, R. Tao, G. Lubineau, Bio-inspired adhesive joint with improved interlaminar fracture toughness, Composites: Part A 149 (2021) 106530.

[9] G. Bao, Z. Suo, Remarks on crack-bridging concepts, Applied Mechanics Reviews 45 (8) (1992) 355–366.

[10] R. B. Sills, M. D. Thouless, Cohesive-length scales for damage and toughening mechanisms, International Journal of Solids and Structures 55 (2015) 32–43.

[11] A. Szekrényes, J. Uj, Advanced beam model for fiber-bridging in unidirectional composite double-cantilever beam specimens, Engineering Fracture Mechanics 72 (2005) 2686–2702.

[12] D. S. Dugdale, Yielding of steel sheets containing slits, Journal of the Mechanics and Physics of Solids 8 (1960) 100–104.

[13] G. I. Barenblatt, The mathematical theory of equilibrium cracks in brittle fracture, Advances in Applied Mechanics 7 (1962) 55–129.

[14] Q. Yang, B. Cox, Cohesive models for damage evolution in laminated composites, International Journal of Fracture 133 (2005) 107–137.

[15] M. A. Gutiérrez, Energy release control for numerical simulations of failure in quasi-brittle solids, Communications in Numerical Methods in Engineering 20 (2004) 19–29.

[16] ISO-15024, Fibre-reinforced plastic composites - determination of mode I interlaminar fracture toughness, GIC, for unidirectionally reinforced materials (2002).

[17] ASTM-D5528, Standard test method for mode I interlaminar fracture toughness of unidirectional fiber-reinforced polymer matrix composites.

[18] C. DiFrancia, T. C. Ward, R. O. Claus, The single-fibre pull-out test. 1: Review and interpretation, Composites: Part A 27A (1996) 597–612.

[19] P. Rossi, P. Acker, Y. Malier, Effect of steel fibres at two different stages: the material and the structure, Materials and Structures 20 (1987) 436–439.

[20] P. Ladevèze, E. Baranger, M. Genet, C. Cluzel, Ceramic Matrix Composites: Materials, Modeling and Technology, Wiley, 2014, Ch. Damage and lifetime modeling for structure computations.

[21] X. Li, S. Lu, G. Lubineau, Snap-back instabilities of double cantilever beam with bridging, International Journal of Solids and Structures 233 (2021) 111150.

[22] A. Carpinteri, R. Massabò, Continuous vs discontinuous bridged-crack models for fiber-reinforced materials in flexure, International Journal of Solids and Structures 34 (18) (1997) 2321–2338.